

Geophysical Research Letters®

RESEARCH LETTER

10.1029/2021GL095443

Key Points:

- Spatial gradients are observed in dilution-corrected mixing ratios of nitrous acid, ozone, and reactive organics in fresh wildfire plumes
- Gradients evolve with time of day, as intensity of chemical aging varies relative to plume transport and mixing
- Gradients should be considered when comparing plume models with measurements and estimating fire emissions from in situ observations

Supporting Information:

Supporting Information may be found in the online version of this article.

Correspondence to:

B. B. Palm,
bbpalm@ucar.edu

Citation:

Palm, B. B., Peng, Q., Hall, S. R., Ullmann, K., Campos, T. L., Weinheimer, A., et al. (2021). Spatially resolved photochemistry impacts emissions estimates in fresh wildfire plumes. *Geophysical Research Letters*, 48, e2021GL095443. <https://doi.org/10.1029/2021GL095443>

Received 29 JUL 2021

Accepted 7 NOV 2021

Author Contributions:

Conceptualization: Brett B. Palm

Data curation: Brett B. Palm, Qiaoyun Peng, Samuel R. Hall, Kirk Ullmann, Teresa L. Campos, Andrew Weinheimer, Deedee Montzka, Geoffrey Tyndall, Wade Permar, Lu Hu, Frank Flocke, Emily V. Fischer

Formal analysis: Brett B. Palm

Funding acquisition: Emily V. Fischer

Investigation: Brett B. Palm, Qiaoyun Peng, Samuel R. Hall, Kirk Ullmann, Teresa L. Campos, Andrew Weinheimer, Deedee Montzka, Geoffrey Tyndall, Wade Permar, Lu Hu, Frank Flocke, Emily V. Fischer












Methodology: Brett B. Palm

Project Administration: Frank Flocke, Emily V. Fischer

Resources: Emily V. Fischer

Writing – original draft: Brett B. Palm

Spatially Resolved Photochemistry Impacts Emissions Estimates in Fresh Wildfire Plumes

Brett B. Palm¹ , Qiaoyun Peng¹, Samuel R. Hall² , Kirk Ullmann² , Teresa L. Campos², Andrew Weinheimer² , Deedee Montzka² , Geoffrey Tyndall² , Wade Permar³ , Lu Hu³ , Frank Flocke² , Emily V. Fischer⁴ , and Joel A. Thornton¹ 

¹Department of Atmospheric Sciences, University of Washington, Seattle, WA, USA, ²Atmospheric Chemistry Observations and Modeling Laboratory, National Center for Atmospheric Research, Boulder, CO, USA, ³Department of Chemistry and Biochemistry, University of Montana, Missoula, MT, USA, ⁴Department of Atmospheric Science, Colorado State University, Fort Collins, CO, USA

Abstract Wildfire emissions affect downwind air quality and human health. Predictions of these impacts using models are limited by uncertainties in emissions and chemical evolution of smoke plumes. Using high-time-resolution aircraft measurements, we illustrate spatial variations that can exist within a plume due to differences in the photochemical environment. Horizontal and vertical crosswind gradients of dilution-corrected mixing ratios were observed in midday plumes for reactive compounds and their oxidation products, such as nitrous acid, catechol, and ozone, likely due to faster photochemistry in optically thinner plume edges relative to darker plume cores. Gradients in plumes emitted close to sunset are characterized by titration of O₃ in the plume and reduced or no gradient formation. We show how crosswind gradients can lead to underestimated emission ratios for reactive compounds and overestimated emission ratios for oxidation products. These observations will lead to improved predictions of wildfire emissions, evolution, and impacts across daytime and nighttime.

Plain Language Summary Wildfire emissions have large impacts on air quality and health in downwind communities. Previous research has shown that chemical reactions in fire plumes can be remarkably fast, which modifies the impact the smoke has downwind. In this work, we show how this chemistry happens faster on the edges versus the core of plumes emitted during midday. For plumes emitted near or after sunset, oxidation chemistry generally slows and remains nearly uniform across the plume. These variations in plume chemistry will impact how plumes are modeled, and how well we can predict downwind air quality impacts.

1. Introduction

Wildfire emissions are becoming increasingly important drivers of degraded air quality, especially in the Western U.S (McClure & Jaffe, 2018; O'Dell et al., 2019). Wildfire season is growing longer and fires are growing larger due to several factors, including climate change, a legacy of fire suppression, and an increasing wildland-urban interface (Abatzoglou & Williams, 2016; Balch et al., 2017; Dennison et al., 2014; Higuera & Abatzoglou, 2021; Higuera et al., 2021; Radeloff et al., 2018; Westerling, 2016). A better understanding of the composition and evolution of wildfire emissions is needed to predict the impacts on downwind communities, atmospheric dynamics, and climate.

In aircraft studies of wildfires and other point sources, emissions are typically evaluated by sampling plume composition in horizontal transects of the plume perpendicular to the wind direction (crosswind transects), where each transect corresponds to a similar physical plume age. A regional background abundance from outside the plume is subtracted from the average crosswind transect abundance to determine a normalized excess mixing ratio (NEMR) for each transect (e.g., Akagi et al., 2012; Liu et al., 2017; Palm et al., 2020; Yokelson et al., 2009). The NEMR values in the youngest parts of the plume are often used as estimates of the emission ratio (ER), which is meant to represent the relative emission flux of a species from the fire prior to any substantial physical or chemical changes with aging. ERs and related emission factors (EF; emission per mass of fuel burned) are essential components of biomass burning emissions inventories used in air quality and earth system models (e.g., Andreae, 2019; van der Werf et al., 2017; Wiedinmyer et al., 2011; Yokelson et al., 1999).

Spatial variations in plume chemistry can make NEMRs (and ERs estimated from them) dependent upon which portion of the crosswind transects are used in the calculation (e.g., entire transect versus plume core), especially

Writing – review & editing: Brett B. Palm, Qiaoyun Peng, Samuel R. Hall, Geoffrey Tyndall, Wade Permar, Lu Hu, Frank Flocke, Emily V. Fischer

for chemically reactive components. Spatial variation in wildfire plume chemistry has rarely been investigated in detail across plume transects (Garofalo et al., 2019; Hodshire et al., 2021; Juncosa Calahorrano et al., 2021; Peng et al., 2020; Wang et al., 2021). Furthermore, vertical gradients in plume chemistry have not been investigated in situ to our knowledge. We use high-time-resolution measurements from a recent flight campaign to investigate horizontal and vertical spatial variation in wildfire plume chemistry. This work shows the importance of considering spatial gradients in oxidation chemistry of fresh wildfire plumes.

2. Materials and Methods

2.1. WE-CAN Campaign

The Western Wildfire Experiment for Cloud Chemistry, Aerosol Absorption, and Nitrogen (WE-CAN) field campaign took place in the Western U.S. July–September 2018. Measurements were taken using a suite of instruments installed aboard a C-130 aircraft operated by the National Center for Atmospheric Research (NCAR) and the National Science Foundation (NSF). The C-130 sampled nearly two dozen individual wildfire plumes, targeting fresh emissions and aging up to several hours. Measurements from the Taylor Creek Fire and the South Sugarloaf Fire plumes are presented below as examples, followed by a broader analysis of all plumes during WE-CAN.

2.2. Plume Measurements

The main instrument used in this analysis was an iodide-adduct high-resolution time-of-flight mass spectrometer (I^- CIMS), measuring a suite of gas-phase oxidized organic and inorganic compounds. The I^- CIMS operation has been described in detail in Palm et al. (2020). More details of the I^- CIMS and other instruments used in this analysis can be found in Text S1 in Supporting Information S1. For this analysis, data from all instruments were smoothed by a 5 s average. Plumes were defined as any data where the enhancement of CO above measured out-of-plume regional backgrounds was greater than 250 ppbv.

NEMR values across transects were calculated by taking the ratio of background-subtracted abundances of each compound to background-subtracted CO using 5 s averaged data. See Text S1 in Supporting Information S1 for more details of background subtraction.

3. Results and Discussion

3.1. Taylor Creek Fire: Narrow Plume With High [HONO]

3.1.1. Gradients in Reactive Compound NEMRs

Early on July 30, 2018, the Taylor Creek fire in southern Oregon emitted smoke into a smoke-filled boundary layer with other nearby fires. Soon after the research aircraft arrived in the area, the fire intensity and environmental conditions supported the injection of a fresh plume above the boundary layer (3.3–3.7 km above sea level; ASL) in the relatively clean free troposphere (see pictures in Figure S1 in Supporting Information S1). The narrow plume (~3–5 km across) was first sampled shortly (~10 min) after it was observed to be injecting into the free troposphere, with an estimated physical age of about 21 min after emission. Because the sampling began shortly after injection, the aircraft was able to continually resample the leading edge of the plume as it aged from 15:45 to 18:00 local time (LT), providing confidence that this was a near-Lagrangian experiment covering approximately 21–140 min physical age (shown in Figure S2d in Supporting Information S1). This plume is presented here as one of the clearest examples of crosswind gradient evolution during WE-CAN.

With the effects of dilution removed by normalizing to excess CO, the horizontal crosswind and downwind NEMR gradients observed for a suite of reactive compounds and oxidation products (Figure 1) were a result of variable rates of chemical loss/production across the plume. Broadly, the variety of observations were consistent with relatively rapid OH oxidation chemistry and near-Lagrangian sampling. For the fastest reacting compounds such as $C_6H_6O_2$ (likely catechol), HONO (nitrous acid), and $C_7H_8O_2$ (likely methyl catechol, shown in Figure S2 in Supporting Information S1), high mixing ratios were observed only in the core of the first several transects closest to the fire. At these locations, the plume core was at its darkest, as confirmed by j_{HONO} . In the earliest two transects, the dilution-corrected production rate of OH from HONO photolysis was faster on the plume edges relative to the core (Figure S2 in Supporting Information S1). Even in the first several transects with 20–30 min

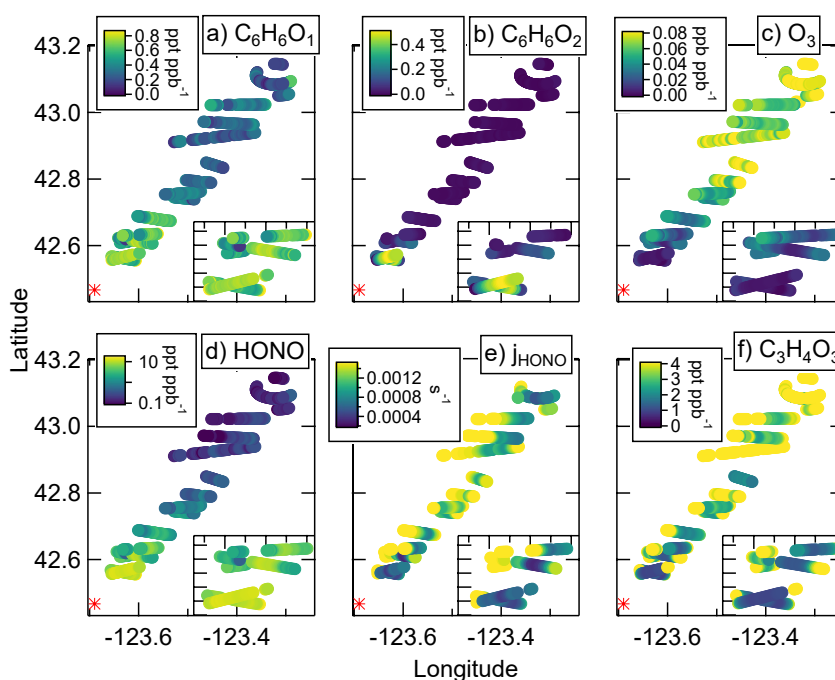


Figure 1. Plume transects of the Taylor Creek fire, showing spatial variations in normalized excess mixing ratios (NEMRs) of (a) $C_6H_6O_1$, (b) $C_6H_6O_2$, (c) O_3 , (d) HONO, (e) j_{HONO} , and (f) $C_3H_4O_3$. The emission source is marked with an asterisk. Insets show the first five transects in greater detail.

physical age, HONO on the plume edges was substantially photolyzed and compounds such as $C_6H_6O_2$ were already mostly reacted away, consistent with expected lifetimes in the low tens of min (Olariu et al., 2000). Slower reacting compounds such as $C_6H_6O_1$ (likely phenol) were depleted more gradually with downwind transport consistent with expected lifetimes of one to several hours (Atkinson et al., 1989), and smaller gradients were observed in the crosswind transects. For compounds that are not reactive on the timescale of several hours of downwind transport, gradients were not observed (or expected) in either the crosswind or downwind directions (e.g., HCN shown in Figure S2 in Supporting Information S1).

For compounds produced from oxidation chemistry, reversed gradients were observed where the compounds were enhanced relative to CO on the plume edges versus the core. This group includes organic oxidation products such as $C_3H_4O_3$ (pyruvic acid and other isomers, as an example of a variety of small organic oxidation products) and ozone (O_3), as shown in Figure 1. A general trend of increasing NEMRs with increasing age downwind was observed for this subset of compounds. In the Taylor Creek plume, near-field O_3 formation was likely influenced by rapid OH chemistry from HONO photolysis during the midday sampling. The Taylor Creek plume contained one of the highest measured HONO ERs of any fire during the campaign (Peng et al., 2020).

3.1.2. Inferred Crosswind Gradients of Average OH Concentrations in Fresh Plumes

The crosswind gradients observed in the NEMRs of reactive compounds and their oxidation products must result from gradients in oxidant concentrations. In the Taylor Creek plume, the large source of OH from HONO photolysis in this relatively bright midday plume meant that OH was likely the dominant oxidant for most compounds. Here, we use the gradients of reactive compounds to infer spatial variations in photochemical aging due to OH oxidation at different locations within the plume.

The average OH radical concentration ($[OH]_{avg}$) experienced by air sampled at any point within the plume since emission can be calculated using Equation 1, derived from de Gouw et al. (2005) and Roberts et al. (1984). We use the known reaction rates of compounds A and B with OH (k_{OH+A} and k_{OH+B} ; see Table S1 in Supporting Information S1 for all rates used), the initial emission ratio of the compounds (at $t = 0$), and the estimated physical time since emission (Δt).

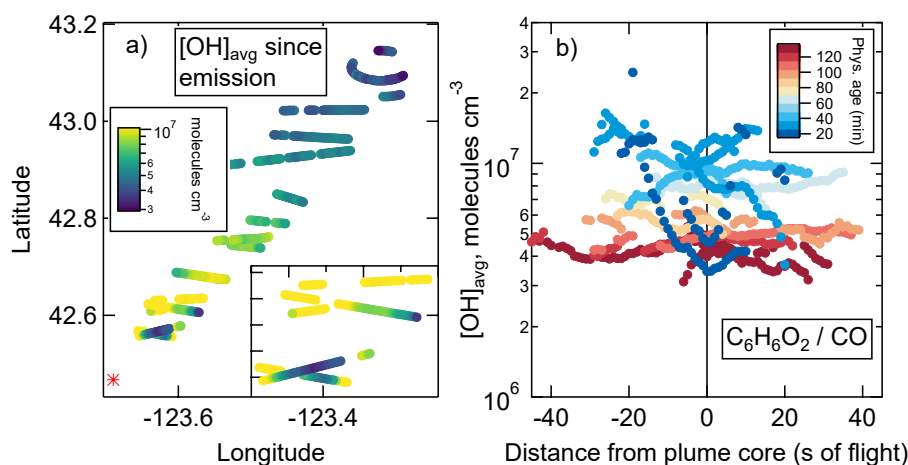


Figure 2. In the Taylor Creek Fire plume, (a) $[\text{OH}]_{\text{avg}}$ between emission source (marked with an asterisk) and each sampled location, and (b) $[\text{OH}]_{\text{avg}}$ between emission source and each sampled location versus distance from plume core defined as maximum $[\text{CO}]$ in each transect. Data are colored by estimated physical age.

$$[\text{OH}]_{\text{avg}} = \frac{1}{\Delta t (k_{\text{OH}+\text{A}} - k_{\text{OH}+\text{B}})} \times \left(\ln \left(\frac{[\text{A}]}{[\text{B}]} \right)_{t=0} - \ln \left(\frac{[\text{A}]}{[\text{B}]} \right) \right) \quad (1)$$

This equation can be rearranged to give OH exposure as well ($\text{OH}_{\text{exp}} = [\text{OH}]_{\text{avg}} \times \Delta t$). Equation 1 is valid when OH is the only relevant oxidant for the chosen compounds during Δt . Compounds **A** and **B** are chosen such that they react with OH at different rates (and are not produced as oxidation products) and their ratio of emissions can be estimated. When $k_{\text{OH}+\text{B}}$ is slow enough that B does not appreciably react during Δt (as is the case for CO), then the sole purpose of compound **B** is to account for dilution, and Equation 1 can be simplified to the exponential decay of dilution-corrected compound **A**. The methodology is further described in Text S2 in Supporting Information S1.

We used $\text{C}_6\text{H}_6\text{O}_2$ and CO as compounds **A** and **B** in Equation 1 to estimate $[\text{OH}]_{\text{avg}}$ experienced by the plume between emission and the point of sampling across each transect, as shown in Figure 2. For $\text{C}_6\text{H}_6\text{O}_2$, the nitrate radical (NO_3) is also a relevant oxidant. Since $k_{\text{OH}+\text{C}_6\text{H}_6\text{O}_2}$ and $k_{\text{NO}_3+\text{C}_6\text{H}_6\text{O}_2}$ are nearly equal (1.0×10^{-10} and $9.9 \times 10^{-11} \text{ cm}^3 \text{ molecule}^{-1} \text{ s}^{-1}$, respectively; Olariu et al., 2000, 2004), Equation 1 provides an estimate of $[\text{OH} + \text{NO}_3]_{\text{avg}}$. Box modeling (Text S2 in Supporting Information S1) suggests approximately 25% of $\text{C}_6\text{H}_6\text{O}_2$ reacts with NO_3 (and negligible reaction with O_3 ; uncertainties discussed in Text S2 in Supporting Information S1) in the Taylor Creek Fire plume. Thus, we multiplied the result of Equation 1 by 0.75 to estimate $[\text{OH}]_{\text{avg}}$ whenever using $\text{C}_6\text{H}_6\text{O}_2$.

In the several transects closest to the fire with estimated physical age of about 20 min, steep crosswind gradients were observed for $[\text{OH}]_{\text{avg}}$ in Figure 2. On the plume edges where HONO photolysis was faster, we inferred $[\text{OH}]_{\text{avg}}$ on the order of $1.0 \times 10^7 \text{ molecules cm}^{-3}$, while the plume core was much lower at approximately $4 \times 10^6 \text{ molecules cm}^{-3}$. In transects further downwind, with physical ages >45 min, the HONO in the center of the transects had also photolyzed, and the $[\text{OH}]_{\text{avg}}$ inferred in the plume center was essentially the same as that of the plume edges near $1.0 \times 10^7 \text{ molecules cm}^{-3}$. The inferred $[\text{OH}]_{\text{avg}}$ (and the gradients of other compounds in Figure 1) became essentially flat across each transect as the plume aged further, decreasing with increasing est. physical age, from $1.0 \times 10^7 \text{ molecules cm}^{-3}$ closer to the fire to $4 \times 10^6 \text{ molecules cm}^{-3}$ after 2 hr of physical aging. These values are the $[\text{OH}]_{\text{avg}}$ between emission and sampling, so the actual $[\text{OH}]$ in the latter part of this plume was lower. OH_{exp} is shown in Figure S4 in Supporting Information S1 for comparison.

The choice of initial ratio of $\text{C}_6\text{H}_6\text{O}_2$ to CO is a potential source of uncertainty. For the calculations above, we used an initial ratio of 1. A sensitivity analysis, discussed in Text S3 in Supporting Information S1, found that the gradients in $[\text{OH}]_{\text{avg}}$ were robust for different initial ratios. Analysis of other compound ratios (Text S3 in Supporting Information S1) illustrates how crosswind $[\text{OH}]_{\text{avg}}$ gradients are only quantifiable because $\text{C}_6\text{H}_6\text{O}_2$ reacts fast enough to form measurable crosswind gradients.

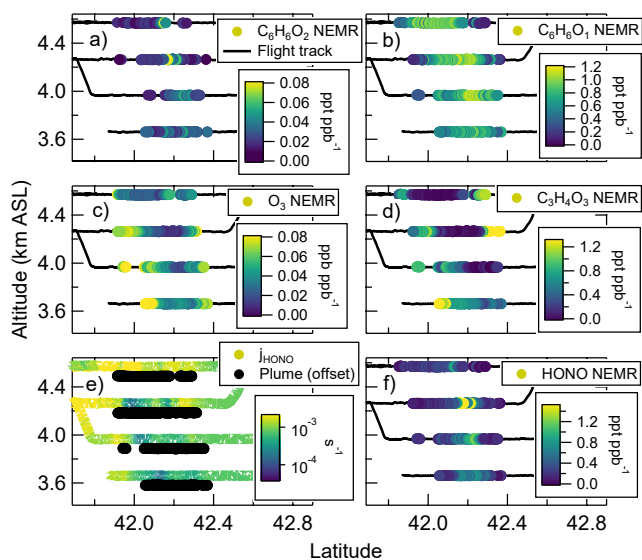


Figure 3. Measurements in four vertically stacked transects of the South Sugarloaf fire, sampled at an average est. physical age of 76 min from 14:50 to 15:50 LT. The plume center is defined by enhanced (a) $C_6H_6O_2$, (b) $C_6H_6O_1$, and (f) HONO. (c) O_3 and (d) $C_3H_4O_3$ are enhanced on the edges, top, and bottom of the plume. Measured (e) j_{HONO} is shown along the entire flight track, with the plume location indicated with offset black dots for comparison.

Since the OH source from HONO in this plume was one of the largest measured during WE-CAN, our estimates likely fall near the upper end of [OH] in fresh plumes from fires in this region. Larger and darker plumes, or plumes emitted near or after sunset, may have stronger influence from other oxidants such as NO_3 or O_3 . However, crosswind gradients were observed in multiple wildfire plumes sampled during WE-CAN, as shown for the South Sugarloaf fire in the next section and for the broader WE-CAN measurements in Section 3.3.

3.2. South Sugarloaf Fire: Vertical Resolution of a Wide Plume

The South Sugarloaf Fire plume, sampled in northern Nevada on 26 August, 2018, differed from the Taylor Creek plume in several ways. The fire was active over a larger area, leading to a plume approaching 100 km wide. The plume remained in the boundary layer and was more than 1 km in height from roughly 3.6–4.6 km ASL. Due to its size and close proximity to the base of operations, this was the only fire during WE-CAN that was sampled with vertically stacked crosswind transects to investigate vertical NEMR gradients (see Figure S7 in Supporting Information S1). The maximum HONO mixing ratios were not as high as Taylor Creek, but were more in line with other fires sampled during WE-CAN (Peng et al., 2020). Also, the HONO photolysis rates were generally slower, in part because this plume was sampled when clouds were present aloft. The clouds were not interacting with the smoke. While the Taylor Creek plume was sampled only during midafternoon, the South Sugarloaf fire was sampled from midday through nearly sunset (14:00–20:00 LT). This more extended sampling allowed an investigation of how vertical and horizontal crosswind gradients evolved as day transitioned to night.

Gradients were observed during midday between the cores and edges of vertically stacked crosswind transects in the South Sugarloaf fire (Figure 3). Compounds such as $C_6H_6O_1$, $C_6H_6O_2$, and HONO were depleted on the edges of each transect, while O_3 and $C_3H_4O_3$ were enhanced. Vertically stacked measurements of HCN, CO, and calculated $[OH]_{avg}$ are shown in Figure S9 for comparison. $[OH]_{avg}$ is again calculated from $C_6H_6O_2$ and CO, shown for comparison with Figure 2 though it may be less reliable due to a larger possible influence from non-OH oxidation chemistry in the darker plume conditions.

NEMR gradients in the vertical were observed as well. HONO was most depleted in the top transect and along the edges, owing to the higher j_{HONO} values in those locations. The highest HONO mixing ratios were found not in the lowest altitude transect as j_{HONO} might suggest, but in the upper middle transect where both j_{HONO} was low and [CO] was high. Either the smoke in the lowest crosswind transects experienced higher j_{HONO} values along their trajectory between emission and being sampled, or the HONO emission factor was higher for smoke that rose to a higher altitude, consistent with more intense combustion conditions being a source of HONO (Peng et al., 2020). While the narrow Taylor Creek plume might reasonably be assumed to have a single emission factor for each compound, the much broader South Sugarloaf Fire likely resulted from a more diverse mix of spatially inhomogeneous emission processes that may not have been well-mixed during transport. Some variation in dilution-corrected HCN was observed, though generally it remained constant across each transect (Figure S9 in Supporting Information S1). Reactive organic compounds such as $C_6H_6O_1$ and $C_6H_6O_2$ followed the trend of HONO of being most concentrated in the core of the plume and depleted at variable rates above, below, and to the sides of that core. O_3 was enhanced in those same locations relative to the core. $C_3H_4O_3$ was enhanced more toward the lower altitudes and on the edges.

Several other vertically stacked transects of the South Sugarloaf Fire plume were conducted at various physical ages and times of day, which further illustrate the variety of possible gradients. These examples, discussed in Text S4 in Supporting Information S1, include two sets of transects sampled at the same estimated physical age of 47 min. One set was sampled during midday and captured strong vertical gradients in the top-most part of the plume (Figure S10 in Supporting Information S1) while the other set was sampled near sunset and showed con-

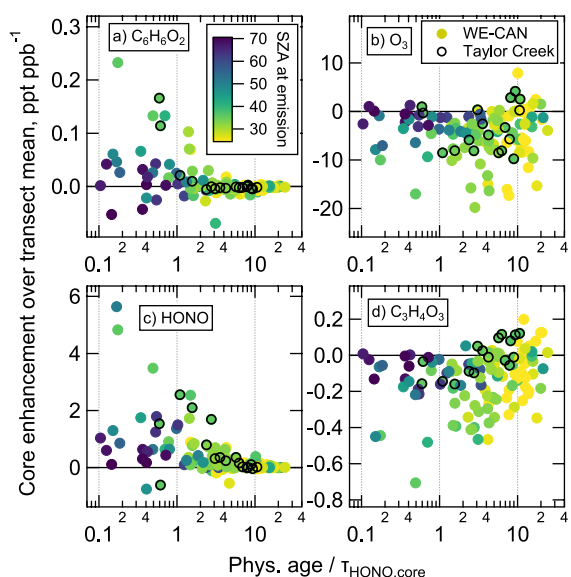


Figure 4. Enhancements of normalized excess mixing ratios (NEMRs) in plume cores (average where $[CO] > 90$ th percentile) relative to transect mean NEMRs for all Western Wildfire Experiment for Cloud Chemistry, Aerosol Absorption, and Nitrogen (WE-CAN) transects, for (a) $C_6H_6O_2$, (b) O_3 , (c) HONO, and (d) $C_3H_4O_3$. The Taylor Creek plume transects are highlighted with black circles.

ditions with O_3 depletion, weaker gradients due to slow HONO photolysis, and some variability that may indicate inhomogeneous emissions or transport (Figure S11 in Supporting Information S1). These examples highlight the need to consider the time of day when wildfire emissions occur.

3.3. Gradient Strength Depends on Time of Day at Emission and Sampling

To investigate the representativeness of the above examples, we performed an analysis of gradients observed in all crosswind transects in coherent plumes (at least three physical ages sampled) sampled during the WE-CAN field campaign with estimated physical ages up to 6 hr. The gradient magnitude was defined as the difference between the NEMR of the plume core (defined as where $[CO]$ was above the 90th percentile in each crosswind transect) versus the transect average NEMR. The above examples suggested that gradients are more tied to the extent of chemical aging rather than physical age. Since chemical aging was driven by OH chemistry from HONO photolysis, this analysis uses a chemical aging metric of the ratio of estimated physical age to the lifetime of HONO against photolysis in the plume core ($\tau_{HONO,core}$), calculated as the inverse of the measured $j_{HONO,core}$ in each transect. Values less than one indicate chemically fresh plumes, where the physical age of the plume is less than the amount of time required to drive OH chemistry by photolyzing HONO to an e-folding. Values larger than one indicate more chemically aged plumes, where HONO photolysis and subsequent OH chemistry has largely occurred at that physical age. This calculation does not take into account the history of $j_{HONO,core}$ between emission and measurement (generally increasing with dilution while decreasing as the sun sets), but still provides a reasonable estimate of relative chemical age for these plumes in the first several hours after emission.

Figure 4 shows the gradient magnitude as a function of this chemical age metric for several compounds, with data also colored by the solar zenith angle (SZA) at the time of emission. Broadly, fast reacting compounds like $C_6H_6O_2$, HONO, and $C_7H_8O_2$ (Figure S12 in Supporting Information S1) showed positive gradients (depleted on edges versus core) in chemically fresh plumes and near zero gradients in aged plumes where the compounds were depleted. Oxidation products like O_3 and $C_3H_4O_3$ tended to have negative gradients (enhanced on edges versus core). Compounds that were reactive but not enough to be fully depleted in the first 6 hr of physical aging, like $C_6H_6O_1$, showed positive gradients across the range of chemical ages, while compounds that were unreactive on these timescales like HCN showed no gradients (as expected; Figure S12 in Supporting Information S1).

Focusing on the chemically fresh plumes where the estimated physical age was less than $\tau_{HONO,core}$, the gradient strengths depended on SZA at emission. The plumes emitted closest to midday with the lowest SZA showed the strongest gradients, positive for reactive compounds and negative for oxidation products. When plumes were emitted late in the day at higher SZA, little to no gradients were observed for all compound types.

Trends are also observed when comparing gradient magnitudes to absolute NEMR magnitudes, as shown in Figure S13 in Supporting Information S1 as a function of physical age. For the fastest reacting compounds with photolysis or reaction lifetimes on the order of 30 min or less (e.g., $C_6H_6O_2$, HONO, and $C_7H_8O_2$), the core NEMR was up to 50% higher than the transect average NEMR in the chemically freshest transects. The core NEMR values in the chemically freshest plumes will most closely represent the true ER values. For compounds that react or form on the timescale of one to several hours (e.g., $C_6H_6O_1$, $C_3H_4O_3$, O_3 , etc.), the core NEMR was typically up to 20% higher or lower, respectively, than the transect average and the gradients lasted out to longer physical ages.

We expect there were other fast reacting or fast forming compounds whose crosswind gradients were not discernable in this campaign because, e.g., the I⁻ CIMS or other instruments could not separate isomers with different gradients, oxidation products rapidly partitioned to the unspiciated particle phase, or artifacts from inlet tubing or ionization interfered with spatial resolution and product identification.

4. Conclusions

By sampling crosswind transects of wildfire plumes at different physical ages and altitudes with high spatial resolution, spatial variations in plume oxidation chemistry were observed during the WE-CAN aircraft campaign. Crosswind NEMR gradients were strongest for the most reactive compounds such as HONO and $C_6H_6O_2$ in the chemically freshest plume transects during midday. In the South Sugarloaf fire, vertical gradients were also observed around the plume core. Gradients appeared to be driven by variations in j_{HONO} on diffuse plume edges or tops versus concentrated plume cores during midday plumes. Inhomogeneity in emissions and transport may have also contributed to spatial NEMR variations, especially when photolysis was slow. During late evening plumes (and likely nighttime plumes) when the photolysis lifetime of HONO became long even on plume edges, gradients due to photochemistry were reduced as the OH oxidation chemistry slowed down. This suggests that the fate of wildfire emissions may be dramatically different depending on the time of day at emission.

Averaging entire transects into single NEMR values may lead to up to 50% underestimated ERs for the most reactive compounds (smaller amounts for less reactive compounds), and overestimated ERs for oxidation products in fresh wildfire plumes. Using screening methods such as using the top percentile of data may be more accurate for some applications, but should be combined with other information including the chemical age of the smoke and possible inhomogeneity of emissions or transport. Plume gradients should also be considered when comparing in situ measurements with 0D plume models.

These comprehensive in situ observations of key differences between daytime and nighttime plume chemical evolution will lead to better predictions of wildfire impacts on downwind air quality.

Data Availability Statement

The data were collected using NSF's Lower Atmosphere Observing Facilities, which are managed and operated by NCAR's Earth Observing Laboratory. WE-CAN data (merge R4) are available at <https://www-air.larc.nasa.gov/cgi-bin/ArcView/firexaq?MERGE=1>.

Acknowledgments

B. B. Palm, Q. Peng, and J. A. Thornton were supported by the US National Science Foundation (NSF; AGS-1652688) and National Oceanic and Atmospheric Administration (NOAA; NA17OAR4310012). This research was supported by the U.S. NSF (AGS-1650786 and AGS-1650275). We thank everyone involved in planning and operations during WE-CAN. This material is based upon work supported by the National Center for Atmospheric Research, which is a major facility sponsored by the NSF under Cooperative Agreement 1852977. The operational and scientific support from NCAR's Earth Observing Laboratory and Research Aircraft Facility is gratefully acknowledged.

References

- Abatzoglou, J. T., & Williams, A. P. (2016). Impact of anthropogenic climate change on wildfire across western US forests. *Proceedings of the National Academy of Sciences of the United States of America*, 113(42), 11770–11775. <https://doi.org/10.1073/pnas.1607171113>
- Akagi, S. K., Craven, J. S., Taylor, J. W., McMeeking, G. R., Yokelson, R. J., Burling, I. R., et al. (2012). Evolution of trace gases and particles emitted by a chaparral fire in California. *Atmospheric Chemistry and Physics*, 12(3), 1397–1421. <https://doi.org/10.5194/acp-12-1397-2012>
- Andreae, M. O. (2019). Emission of trace gases and aerosols from biomass burning—An updated assessment. *Atmospheric Chemistry and Physics*, 19(13), 8523–8546. <https://doi.org/10.5194/acp-19-8523-2019>
- Atkinson, R., Baulch, D. L., Cox, R. A., Hampson, R. F., Kerr, J. A., & Troe, J. (1989). Evaluated kinetic and photochemical data for atmospheric chemistry: Supplement III. IUPAC Subcommittee on gas kinetic data evaluation for atmospheric chemistry. *Journal of Physical and Chemical Reference Data*, 18(2), 881–1097. <https://doi.org/10.1063/1.555832>
- Balch, J. K., Bradley, B. A., Abatzoglou, J. T., Nagy, R. C., Fusco, E. J., & Mahood, A. L. (2017). Human-started wildfires expand the fire niche across the United States. *Proceedings of the National Academy of Sciences of the United States of America*, 114, 2946–2951. <https://doi.org/10.1073/pnas.1617394114>
- Burkholder, J. B., Sander, S. P., Abbatt, J., Barker, J. R., Cappa, C., Crounse, J. D., et al. (2019). *Chemical kinetics and photochemical data for use in atmospheric studies*. (Evaluation No. 19, JPL Publication 19-5). Jet Propulsion Laboratory. Retrieved from <http://jpldataeval.jpl.nasa.gov/>
- Decker, Z. C. J., Zarzana, K. J., Coggon, M., Min, K.-E., Pollack, I., Ryerson, T. B., et al. (2019). Nighttime chemical transformation in biomass burning plumes: A box model analysis initialized with aircraft observations. *Environmental Science & Technology*, 53(5), 2529–2538. <https://doi.org/10.1021/acs.est.8b05359>
- de Gouw, J. A., Middlebrook, A. M., Warneke, C., Goldan, P. D., Kuster, W. C., Roberts, J. M., et al. (2005). Budget of organic carbon in a polluted atmosphere: Results from the New England Air Quality Study in 2002. *Journal of Geophysical Research*, 110, D16305. <https://doi.org/10.1029/2004JD005623>
- Dennison, P. E., Brewer, S. C., Arnold, J. D., & Moritz, M. A. (2014). Large wildfire trends in the western United States, 1984–2011. *Geophysical Research Letters*, 41, 2928–2933. <https://doi.org/10.1002/2014GL059576>
- Garofalo, L. A., Pothier, M. A., Levin, E. J. T., Campos, T., Kreidenweis, S. M., & Farmer, D. K. (2019). Emission and evolution of submicron organic aerosol in smoke from wildfires in the Western United States. *ACS Earth and Space Chemistry*, 3(7), 1237–1247. <https://doi.org/10.1021/acsearthspacechem.9b00125>
- Higuera, P. E., & Abatzoglou, J. T. (2021). Record-setting climate enabled the extraordinary 2020 fire season in the western United States. *Global Change Biology*, 27(1), 1–2. <https://doi.org/10.1111/gcb.15388>
- Higuera, P. E., Shuman, B. N., & Wolf, K. D. (2021). Rocky Mountain subalpine forests now burning more than any time in recent millennia. *Proceedings of the National Academy of Sciences of the United States of America*, 118, e2103135118. <https://doi.org/10.1073/pnas.2103135118>
- Hodshire, A. L., Ramnarine, E., Akherati, A., Alvarado, M. L., Farmer, D. K., Jathar, S. H., et al. (2021). Dilution impacts on smoke aging: Evidence in Biomass Burning Observation Project (BBOP) data. *Atmospheric Chemistry and Physics*, 21(9), 6839–6855. <https://doi.org/10.5194/acp-21-6839-2021>

- Jenkin, M. E., Young, J. C., & Rickard, A. R. (2015). The MCM v3.3.1 degradation scheme for isoprene. *Atmospheric Chemistry and Physics*, 15(20), 11433–11459. <https://doi.org/10.5194/acp-15-11433-2015>
- Joo, T., Rivera-Rios, J. C., Takeuchi, M., Alvarado, M. J., & Ng, N. L. (2019). Secondary organic aerosol formation from reaction of 3-methylfuran with nitrate radicals. *ACS Earth and Space Chemistry*, 3(6), 922–934. <https://doi.org/10.1021/acsearthspacechem.9b00068>
- Juncosa Calahorrano, J. F., Lindaas, J., O'Dell, K., Palm, B. B., Peng, Q., Flocke, F., et al. (2021). Daytime oxidized reactive nitrogen partitioning in Western U.S. wildfire smoke plumes. *Journal of Geophysical Research: Atmospheres*, 126, e2020JD033484. <https://doi.org/10.1029/2020JD033484>
- Liu, X., Huey, L. G., Yokelson, R. J., Selimovic, V., Simpson, I. J., Müller, M., et al. (2017). Airborne measurements of western U.S. wildfire emissions: Comparison with prescribed burning and air quality implications. *Journal of Geophysical Research: Atmospheres*, 122, 6108–6129. <https://doi.org/10.1002/2016JD026315>
- McClure, C. D., & Jaffe, D. A. (2018). US particulate matter air quality improves except in wildfire-prone areas. *Proceedings of the National Academy of Sciences of the United States of America*, 115(31), 7901–7906. <https://doi.org/10.1073/pnas.1804353115>
- O'Dell, K., Ford, B., Fischer, E. V., & Pierce, J. R. (2019). Contribution of wildland-fire smoke to US PM 2.5 and its influence on recent trends. *Environmental Science & Technology*, 53(4), 1797–1804. <https://doi.org/10.1021/acs.est.8b05430>
- Olariu, R. I., Barnes, I., Becker, K. H., & Klotz, B. (2000). Rate coefficients for the gas-phase reaction of OH radicals with selected dihydroxybenzenes and benzoquinones. *International Journal of Chemical Kinetics*, 32(11), 696–702. [https://doi.org/10.1002/1097-4601\(2000\)32:11<696::AID-KINS>3.0.CO;2-N](https://doi.org/10.1002/1097-4601(2000)32:11<696::AID-KINS>3.0.CO;2-N)
- Olariu, R. I., Bejan, I., Barnes, I., Klotz, B., Becker, K. H., & Wirtz, K. (2004). Rate coefficients for the gas-phase reaction of NO₃ radicals with selected dihydroxybenzenes. *International Journal of Chemical Kinetics*, 36(11), 577–583. <https://doi.org/10.1002/kin.20029>
- Palm, B. B., Liu, X., Jimenez, J. L., & Thornton, J. A. (2019). Performance of a new coaxial ion–molecule reaction region for low-pressure chemical ionization mass spectrometry with reduced instrument wall interactions. *Atmospheric Measurement Techniques*, 12(11), 5829–5844. <https://doi.org/10.5194/amt-12-5829-2019>
- Palm, B. B., Peng, Q., Fredrickson, C. D., Lee, B. H., Garofalo, L. A., Pothier, M. A., et al. (2020). Quantification of organic aerosol and brown carbon evolution in fresh wildfire plumes. *Proceedings of the National Academy of Sciences of the United States of America*, 117(47), 29469–29477. <https://doi.org/10.1073/pnas.2012218117>
- Peng, Q., Palm, B. B., Melander, K. E., Lee, B. H., Hall, S. R., Ullmann, K., et al. (2020). HONO emissions from Western U.S. wildfires provide dominant radical source in fresh wildfire smoke. *Environmental Science & Technology*, 54(10), 5954–5963. <https://doi.org/10.1021/acs.est.0c00126>
- Radeloff, V. C., Helmers, D. P., Kramer, H. A., Mockrin, M. H., Alexandre, P. M., Bar-Massada, A., et al. (2018). Rapid growth of the US wildland-urban interface raises wildfire risk. *Proceedings of the National Academy of Sciences of the United States of America*, 115(13), 3314–3319. <https://doi.org/10.1073/pnas.1718850115>
- Roberts, J. M., Fehsenfeld, F. C., Liu, S. C., Bollinger, M. J., Hahn, C., Albritton, D. L., & Sievers, R. E. (1984). Measurements of aromatic hydrocarbon ratios and NO_x concentrations in the rural troposphere: Observation of air mass photochemical aging and NO_x removal. *Atmospheric Environment*, 18(11), 2421–2432. [https://doi.org/10.1016/0004-6981\(84\)90012-X](https://doi.org/10.1016/0004-6981(84)90012-X)
- Shetter, R. E., & Müller, M. (1999). Photolysis frequency measurements using actinic flux spectroradiometry during the PEM-Tropics mission: Instrumentation description and some results. *Journal of Geophysical Research*, 104(D5), 5647–5661. <https://doi.org/10.1029/98JD01381>
- van der Werf, G. R., Randerson, J. T., Giglio, L., van Leeuwen, T. T., Chen, Y., Rogers, B. M., et al. (2017). Global fire emissions estimates during 1997–2016. *Earth System Science Data*, 9(2), 697–720. <https://doi.org/10.5194/essd-9-697-2017>
- Wang, S., Coggon, M. M., Gkatzelis, G. I., Warneke, C., Bourgeois, I., Ryerson, T., et al. (2021). Chemical tomography in a fresh wildland fire plume: A Large Eddy Simulation (LES) study. *Journal of Geophysical Research: Atmospheres*, 126, e2021JD035203. <https://doi.org/10.1029/2021JD035203>
- Westerling, A. L. (2016). Increasing western US forest wildfire activity: Sensitivity to changes in the timing of spring. *Philosophical Transactions of the Royal Society B: Biological Sciences*, 371(1696), 20150178. <https://doi.org/10.1098/rstb.2015.0178>
- Wiedinmyer, C., Akagi, S. K., Yokelson, R. J., Emmons, L. K., Al-Saadi, J. A., Orlando, J. J., & Soja, A. J. (2011). The Fire INventory from NCAR (FINN): A high resolution global model to estimate the emissions from open burning. *Geoscientific Model Development*, 4(3), 625–641. <https://doi.org/10.5194/gmd-4-625-2011>
- Wolfe, G. M., Marvin, M. R., Roberts, S. J., Travis, K. R., & Liao, J. (2016). The Framework for 0-D Atmospheric Modeling (FOAM) v3.1. *Geoscientific Model Development*, 9(9), 3309–3319. <https://doi.org/10.5194/gmd-9-3309-2016>
- Yokelson, R. J., Crouse, J. D., DeCarlo, P. F., Karl, T., Urbanski, S., Atlas, E., et al. (2009). Emissions from biomass burning in the Yucatan. *Atmospheric Chemistry and Physics*, 9(15), 5785–5812. <https://doi.org/10.5194/acp-9-5785-2009>
- Yokelson, R. J., Goode, J. G., Ward, D. E., Susott, R. A., Babbitt, R. E., Wade, D. D., et al. (1999). Emissions of formaldehyde, acetic acid, methanol, and other trace gases from biomass fires in North Carolina measured by airborne Fourier transform infrared spectroscopy. *Journal of Geophysical Research*, 104(D23), 30109–30125. <https://doi.org/10.1029/1999JD900817>

References From the Supporting Information

- Atkinson, R., & Arey, J. (2003). Atmospheric degradation of volatile organic compounds. *Chemical Reviews*, 103(12), 4605–4638. <https://doi.org/10.1021/cr0206420>
- Coggon, M. M., Lim, C. Y., Koss, A. R., Sekimoto, K., Yuan, B., Gilman, J. B., et al. (2019). OH chemistry of non-methane organic gases (NMOGs) emitted from laboratory and ambient biomass burning smoke: Evaluating the influence of furans and oxygenated aromatics on ozone and secondary NMOG formation. *Atmospheric Chemistry and Physics*, 19(23), 14875–14899. <https://doi.org/10.5194/acp-19-14875-2019>
- Lebague, B., Schmidt, M., Ramonet, M., Wastine, B., Yver Kwok, C., Laurent, O., et al. (2016). Comparison of nitrous oxide (N₂O) analyzers for high-precision measurements of atmospheric mole fractions. *Atmospheric Measurement Techniques*, 9(3), 1221–1238. <https://doi.org/10.5194/amt-9-1221-2016>
- Permar, W., Wang, Q., Selimovic, V., Wielgasz, C., Yokelson, R. J., Hornbrook, R. S., et al. (2021). Emissions of trace organic gases from Western U.S. wildfires based on WE-CAN aircraft measurements. *Journal of Geophysical Research: Atmospheres*, 126, e2020JD033838. <https://doi.org/10.1029/2020JD033838>